Construction phasing of a dam spillway: thermo-mechanical simulation

M. Azenha, R.M. Lameiras, J. Barros, A. Costa

ISISE, Institute for Sustainability and Innovation in Structural Engineering
University of Minho, Guimarães, Portugal

SSCS 2012 Numerical Modeling Strategies for Sustainable Concrete Structures
Aix-en-Provence, France
May 29-June 1, 2012

Abstract

One of the most important issues to be taken into account while defining the construction phasing of massive elements, such as dams or thick walls, is the height of each construction stage. In fact, if the height of casting of each construction stage is increased, the temperature variations associated to heat of hydration are raised, with a consequent increase of concrete cracking risk. On the other hand, if the height of each construction phase is reduced, overall construction schedules are penalized, and costs are increased. The thickness of the concrete elements to be cast in each stage should be then as large as possible without causing thermal cracks. The evaluation of alternative construction scenarios and their cracking risk can be assessed with thermo-mechanical models. This paper aims to present an application of thermo-mechanical modeling to the central wall of a dam spillway entrance. The case study has added interest in view of the extensive material characterization, in-situ monitoring of temperature/strain, and the use of air-cooled pipes to reduce temperature increase in concrete.

1. Introduction

The construction phasing of massive concrete elements is an issue that frequently raises doubts to practitioner engineers in regard to the risks of thermal cracking. A sustained estimation of temperature and self-induced stress development that occurs at early ages can only be achieved by numerical simulation with thermo-mechanical models, through which scenarios of construction phasing/scheduling can be compared. Such numerical simulation tools, as support to decision-making, can help to take important decisions about the acceleration of construction phasing, while maintaining early cracking risk under acceptable levels. The acceleration of construction brings important benefits in terms of cost-effectiveness, and increases the overall sustainability of construction.

A thermo-mechanical simulation consists on the initial computation of the temperature field, and subsequent evaluation of the corresponding stresses. The thermal field is calculated considering the variable environmental temperature, the exothermal and thermally activated nature of cement hydration reactions, as well as the adequate modelling of boundary conditions. The stress field is determined for each time step considering the corresponding temperature variation and the thermal dilation coefficient of concrete. The evolution of E-modulus, tensile strength and the creep behaviour at early ages are of particularly importance, and are also carefully estimated.

This paper deals with the assessment of the temperature and stress development in the construction of a 27.5m long wall integrated in a dam spillway, with a thickness that attains a maximum of 2.8m. This wall has a total height of 15m, and is constructed by stages. Particular attention is devoted to a segment of the construction, in which a 2.5m tall concreting was performed, and internal cooling of concrete was made with recourse to prestressing sheaths into which air was blown by industrial fans. Parts of this casting phase were monitored by temperature sensors (thermocouples and thermistors) and vibrating wire strain gages.

The paper encompasses an initial description of the studied structure, along with the corresponding environmental conditions. A brief description of the monitoring system to measure temperatures and

strains is also done. A summary discussion of laboratory characterization tests is made, and the overall properties of the studied concrete are provided. Afterwards, focus is given to the description of modelling strategies and the interpretation of the obtained results, taking into account the available laboratory test data and the in-situ conditions of the spillway wall.

2. Thermo-mechanical modelling

This section deals with a brief description of the numerical strategy adopted. It is organized in two sub-sections that respectively regard the temperature calculations (including the hydration reaction field) and the mechanical analysis. The approach adopted in this research matches the one described in [1], and thus the reader is redirected for such reference for further details about the models/implementation.

2.1. Thermal analysis

Temperature calculation in concrete is made through the equation of transient thermal equilibrium in homogeneous isotropic continuous media, which allows calculating temperature distribution T in concrete taking into account the thermal conductivity k, the volumetric specific heat ρc and the internal heat generation rate, $\dot{Q}$, caused by cement hydration.

$$k\,\nabla\cdot(\nabla T) + \dot{Q} = \rho c\,\dot{T} \tag{1}$$

Usual approaches in temperature field computation [2, 3] tend to consider that k and ρc are constant throughout the analyses, even though it has been acknowledged that these properties suffer changes along hydration, with a starting value that decreases about 10% and 15% along maturing for k and ρc, respectively [4]. However, parametric analyses conducted reported in [1] have shown that the effect of considering evolutionary values for k and ρc along hydration does not significantly affect the computed temperature field, thus justifying the plausibility of assuming these properties with constant value.

To evaluate $\dot{Q}$ an Arrhenius-type equation is adopted [5],

$$\dot{Q} = A\, f(\alpha)\, e^{-\frac{E_a}{R(273.15+T)}} \tag{2}$$

where T is expressed in ºC, α is the degree of heat development and is computed at each instant t (in each node) by the quotient between the heat generated so far $Q(t)$ and the total heat that would be generated upon completion of hydration reactions Q_{pot}; $f(\alpha)$ is the normalized heat generation function that provides information about chemical reactivity along hydration; A is proportional to the maximum heat generation rate $\dot{Q}_{\max}$ ($\dot{Q}_{\max}$ can be obtained through multiplication of A by the exponential term in equation (2)); E_a is the activation energy; and R is the Universal Gas Constant (8.314 J mol^{-1} K^{-1}). In order to obtain data for equation (2), calorimetric testing is usually required. The work reported here takes advantage of the extensive experimental programme of calorimetric characterization of Portuguese cements reported in [1]. Such experimental programme involved the analysis of 11 cements (marketed by two major Portuguese cement production companies) in an isothermal conduction calorimeter at several temperatures (20ºC, 30ºC, 40ºC, 50ºC and 60ºC), and the treatment of the corresponding data, which resulted in tables of data for equation (2) for concretes containing the cements marketed in Portugal.

The spatial resolution of equation (1) requires accounting for the thermal fluxes occurring at the boundaries between concrete and the surrounding environment. Such thermal fluxes q_T can be evaluated by a convection/radiation boundary condition:

$$q_T = h_{cr}\left(T_b - T_e\right) \tag{3}$$

where T_b is the temperature of concrete at the boundary and T_e is the environmental temperature. The convection/radiation coefficient h_{cr} combines the effect of convection and radiation (radiation

transmission equation was linearized and adjoined to convection flow), and can be assessed by an estimate of the average wind speed [6, 7]. Boundary effects of solar radiation, night cooling and evaporative cooling are disregarded in the present work in view of their limited effect on massive structures. It should however be remarked that the accuracy of surface cracking estimations is negatively affected by such simplifications.

2.2. Mechanical analysis

The stress calculations are made with standard procedures for transient simulation of mechanical behaviour of hardened concrete. Nonetheless, since a multi-physics simulation is being carried out (i.e. temperature fields have been explicitly calculated) and concrete at early ages has certain specificities, some adaptations have to be made. Firstly, the thermal strains are calculated with basis on the computed temperatures and the thermal dilation coefficient (TDC). Even though it has been reported that TDC endures evolution at early ages [8], starting with higher value when concrete is still fresh, few works exist that provide clear information about such evolution. In fact, the experimental procedure to measure TDC at early ages poses many problems, and doubts arise about the accuracy of measurements. As a consequence, distinct types of evolution are reported by different authors [9, 10]. However, all authors tend to be coherent in one aspect: by the age of ~15 hours, the value of TDC is reasonably similar to the value expected for hardened concrete. Therefore, the errors associated to considering constant thermal dilation coefficient in numerical simulations are deemed acceptably low for the calculation of the early age stresses, as long as the E-modulus of concrete is still very low within the period in which TDC evolves. Therefore, it was decided to maintain the TDC with constant value in the numerical analyses.

Another topic of importance in the mechanical analyses of concrete at early ages is the necessity of accurately pinpoint the evolution of mechanical properties (namely the E-modulus and tensile strength), which are naturally influenced by the developed temperatures (thermally activated hydration reactions). Therefore, a strategy based on the equivalent age t_{eq} concept is followed in regard to a given reference temperature T_{ref}:

$$t_{eq} = \int_0^t e^{-\frac{E_a}{R}\left(\frac{1}{273.15+T(\tau)} - \frac{1}{273.15+T_{ref}}\right)} d\tau \tag{4}$$

where t stands for the instant of time where t_{eq} means to be calculated.

The viscoelastic behaviour of concrete at early ages is more pronounced than that of hardened concrete. For such reason, it is often necessary to use creep laws that are specially devised for the analysis of concrete at early ages, and whose parameters are usually fixed upon experimental analysis of the actual concrete being used. The present research has adopted the Double Power Law [11] that has shown adequate predictive performance in previous applications [12, 13]. The corresponding compliance function J is formulated as:

$$J(t,\tau) = \frac{1}{E_0(\tau)} + \frac{\phi_1}{E_0(\tau)}\,\tau^{-m}\,(t-\tau)^n \tag{5}$$

where τ is the age at load application, $E_0(\tau)$ is the asymptotic E-modulus upon loading, ϕ_1 is the creep coefficient and m, n are material parameters.

3. Dam spillway: General description and monitoring

3.1. Overview

The dam spillway under study has been recently built in the North of Portugal, and the work reported here pertains to the construction phasing of the central wall of the spillway at the level of its intake. The wall is 27.5m long, 15m tall and has variable thickness (with a maximum value of 2.8m) – see plan and longitudinal cross section in Figure 1. Therefore the construction had to be performed by stages, which generally corresponded to casting phases of 1.2m height (limitation posed by the owner, based on previous experience). However, at the 21st construction phase there was a demand for having a taller concreting height of 2.5m due to the embedment of steel parts of a sluice gate within the height of the concreting phase. The larger volume of concrete involved causes higher temperatures in

concrete, and thus a greater cracking risk is expectable. To minimize such cracking risk it was decided to implement a cooling system based on air circulation inside prestressing sheaths of 90mm inner diameter. Such kind of cooling system was inspired on the work reported by Hedlund [14] in which vertically placed air-cooled tubes were placed inside thick columns to minimize hydration heat development. However, due to formwork-related limitations, in the present case it was decided to place the cooling tubes in horizontal position.

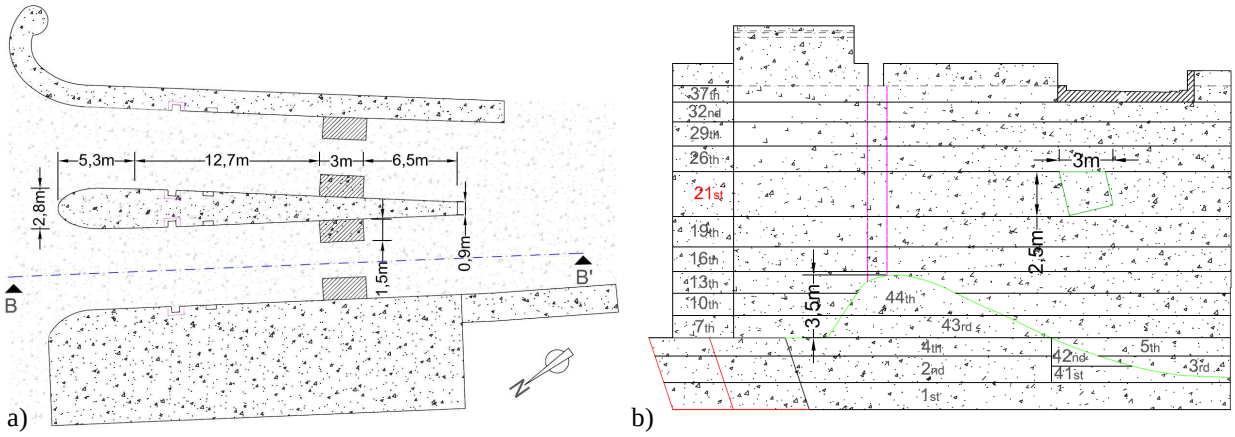

Figure 1: Central wall of the spillway: a) plan; b) longitudinal cross section B-B'

A total of six tubes were placed according to the disposition shown in Figure 2 for the 21st construction phase, and they were dully sealed with cement paste after the cooling process. An industrial fan was placed on the downstream extremity of the tubes, blowing air inside at a measured speed of ~8.6 m/s. No specific cooling measures were taken in regard to the blown air. The fan was only turned on 14h after casting (i.e. well after setting) in order to avoid deleterious effects associated to concrete re-vibration caused by operation of the fan.

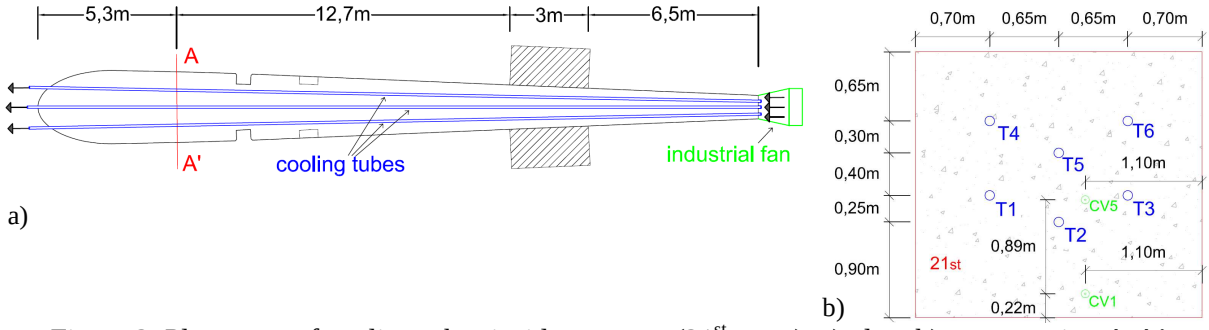

Figure 2: Placement of cooling tubes inside concrete (21st stage): a) plan; b) cross section A-A' (T_i= cooling tube; CV_i = thermal resistive sensor and strain gage)

3.2. Materials and characterization

The majority of the 21st construction phase has been built with C30/37 concrete according to EN1992 [15], and the corresponding composition is shown in Table 1. It should however be remarked that the concrete placed at the embedment of the sluice gate had smaller aggregate size (due to reinforcement density), but a quite similar cement content (280 kg/m^3).

Table 1: Concrete composition of the 21st construction phase

Component	Gravel 14/32	Gravel 10/16	Gravel 4/8	Sand 0/8	CEM I 42,5 R	Fly Ash	Pozzolith 390S	Water
Quantity (kg/m³)	449.00	438.00	306.00	621.00	224.00	96.00	2.20	170.00

It was not possible to conduct laboratory calorimetric characterization for the concrete used in this wall (e.g. semi-adiabatic or adiabatic testing). However, data of cement heat generation from the recent comprehensive study of the cements marketed in Portugal [1] has been used. Such information

allows a reasonable estimate of the heat generation of the concrete used in the wall by mere multiplication of the expectable thermal output of the cement paste (given in [1] as a function of the mass of cement in the paste) by the volumetric content of cement in the concrete. Therefore, the necessary data for simulating the thermal output of concrete was computed and the resulting parameters for application in equation (2) are: E_a = 37.31 kJ/mol, A = 4.989×10^{9}W/m^3, Q_{pot} = 8.295×10^{7}J/m^3, and function $f(\alpha)$ characterized by the following set of data [α; f(α)] = [0.00; 0.00], [0.05; 0.58], [0.10; 0.85], [0.15; 0.98], [0.20; 1.00], [0.30; 0.94], [0.40; 0.69], [0.50; 0.41], [0.60; 0.22], [0.70; 0.13], [0.80; 0.07], [0.90; 0.02], [1.00; 0.00].

Concerning the concrete mechanical characterization, several cubes (15cm edge – for compressive strength evaluation) and cylinders (15cm diameter and 30cm tall) were cast to evaluate the evolution of compressive strength, tensile strength (splitting test) and E-modulus at several ages, under wet curing and at 20ºC temperature. The evolution of compressive strength ($f_{c,cubes}$), tensile strength ($f_{ct,sp}$) and E-modulus (E) along time is given in the following list [t (days); $f_{c,cubes}$ (MPa); $f_{ct,sp}$ (MPa); E (GPa)]=[1; 6.74; -; 14.7]; [2; -; 1.4; -];[3; 19.99; -; 20.9]; [7; 29.92; 2.1; 25.6]; [15; -; -; 26.3]; [29; 42.3; 2.6; 28.6]. Further test specimens were considered in order to assess the feasibility of the equivalent age concept forwarded in equation (4) for the evolution of mechanical properties, and evaluate if the activation energy obtained by calorimetry testing can be used for mechanical properties estimation. Therefore, twelve more cubes were cast and placed in a 40ºC water bath in order to assess the mechanical activation energy based on compressive strength tests at several ages. By applying the superposition method [16], the mechanical activation energy can be evaluated with basis on the result of compressive strength for curing at 20ºC and 40ºC. The computed activation energy was of 37.0 kJ/mol, which is rather consistent with the value of 37.31 kJ/mol forwarded for the thermal activation energy reported above (based on calorimetry data). Compressive creep tests were also carried out (basic creep) for the loading ages of 1, 3 and 7 days, and the resulting parameters for creep estimation according to equation (5) were: ϕ_1=2.15; m=0.48; n=0.19.

3.3. In-situ experiments and monitoring

3.3.1 Heat of hydration assessment

As no laboratory tests were made regarding heat of hydration of the concrete used in the wall, it was decided to make a simple semi-adiabatic calorimeter in-situ. Such semi-adiabatic calorimeter consisted in a concrete cube of 30 cm edge, cast inside a box made of extruded polystyrene foam (XPS) and wood according to the scheme of Figure 3a. The monitored temperatures inside the cube are shown in Figure 3b. These results will be used as a validation for the heat generation rate parameters mentioned in the previous section. The corresponding numerical simulation is relegated to section 4.1 of this paper.

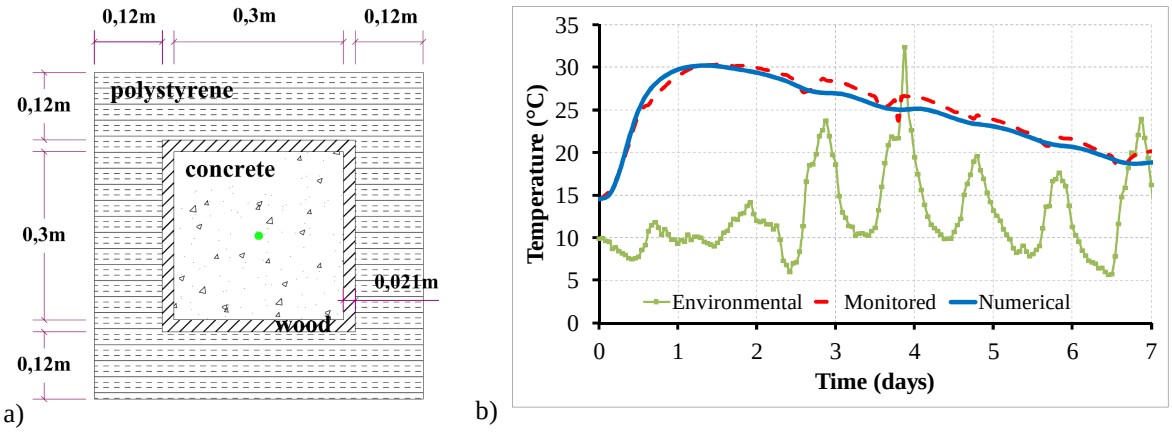

Figure 3: Custom semi-adiabatic calorimeter placed in-situ. a) schematic representation; b) monitored temperature at the centre

3.3.2 Continuous E-modulus measurement

A new methodology for continuous measurement of concrete E-modulus since the instant of casting, named EMM-ARM ('Elasticity Modulus Measurement through Ambient Response Method'), has been recently proposed by Azenha *et al.*[17]. Such methodology consists in the continuous modal identification of the resonant frequency of a composite beam made of a form with known stiffness (e.g. acrylic or steel) and geometry, into which fresh concrete is poured. Along hydration, the resonant frequency of the composite beam is increased due to the increasing stiffness of concrete. Therefore, based on the equations of motion of the beam it is possible to calculate the E-modulus of concrete. The original version of the method has been improved for re-usability and ease of use [18] and it has been applied to the characterization of the E-modulus evolution of the concrete used in the wall – see photo of the test setup in Figure 4a. Further details on this experimental methodology and its description in the scope of this application are given elsewhere [19]. The results of this experimental technique are shown in Figure 4b, where the corresponding results obtained from cyclic compressive tests in cylinders are also depicted. The obtained coherence shows good prospects for the application of EMM-ARM with the purpose of obtaining adequate stiffness estimates at very early ages, which is fundamental for accurate numerical simulation of early stress development.

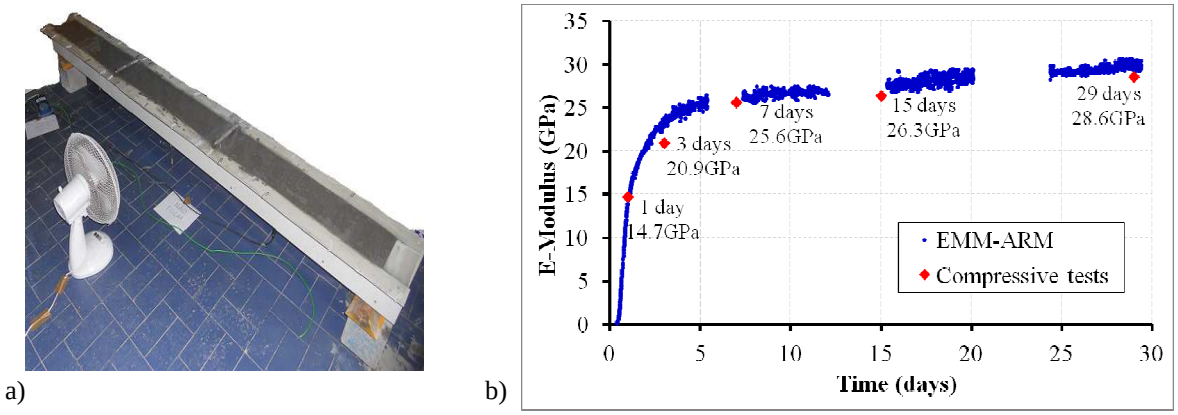

Figure 4: EMM-ARM tests: a) photo; b) results compared to compressive tests

3.3.1 Monitoring of temperatures and strains

Twenty temperature sensors (thermocouples type K and resistive sensors) and seven strain sensors (vibrating wire strain gages) were applied in situ at the 21st construction phase. Most of these sensors were placed near the thickest part of the wall, in section A-A' as labelled in Figure 2a. The layout of some of the most relevant sensors in section A-A' is shown in Figure 2b, and the strain measurements were taken in the longitudinal direction of the wall. Data logging was made at a sampling rate of one measurement in all sensors per 30 minutes (at least). The most relevant results will be shown in section 4.2 upon comparison with the numerical simulation, but all the data is available in [19].

4. Numerical simulation

4.1. Thermal simulation of the semi-adiabatic experiment in-situ

The numerical simulation of the temperatures developed in the semi-adiabatic calorimeter described in section 3.3.1 is shown here. A 3D thermal analysis of the concrete cube with the finite element method has been carried out. As the thickness of the surrounding polystyrene and wood is significant, the simplification of considering them lumped into an equivalent convection coefficient would be unacceptable since it would cause important deviations in results. Therefore, it was decided to explicitly model the polystyrene and wood in the finite element model. Eight node solid elements were used with 2 x 2 x 2 integration points. Due to the double symmetry of the experiment, only one fourth of the specimen and form was modelled. The resulting geometry of the FE model is shown in Figure 5a, whereas the values of the main parameters used for the numerical simulation are shown in Figure 5b. The thermal conductivity and specific heat have been obtained by averaging the corresponding values of the components of the mix [19]. For the convection/radiation coefficient, the adopted value of 15 W m^{-2} K^{-1} is considered reasonable in view of an estimated average wind speed of 2.5 m/s

according to the relationships reported in [1]. The environmental temperature was taken from a temperature sensor placed in-situ and used as input data for the convective boundaries. Solar radiation and night cooling could be disregarded due to the location of the calorimeter (no direct line of sight to the sky). The numerical simulation was carried out for a total of 168 hours with time steps of 1 hour. The calculated temperature development is compared at the monitored point in Figure 3b. A rather good coherence is found, indicating that the use of the heat generation parameters (namely A, $f(\alpha)$,Q_{pot} and E_a) indicated in section 3.2 is feasible for use in the actual concrete of this construction. The good coherence also indicates that reasonable estimates have been taken for k and ρc, as well as for the boundary convection coefficients.

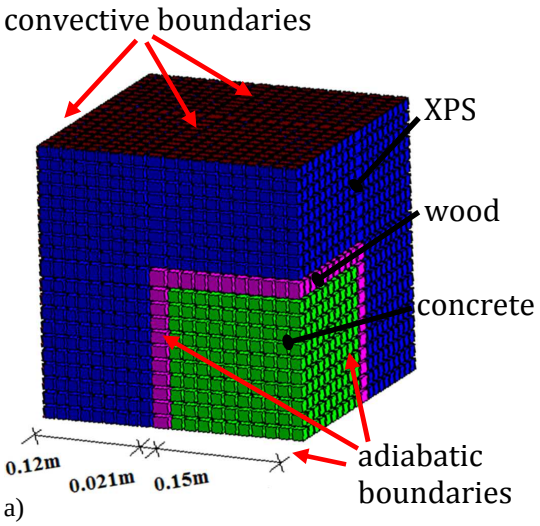

a)

	Concrete	Wood	XPS
$k\ (W/m^2K)$	2.400	0.150	0.035
$\rho c\ (J/m^3K)$	2.4000E+06	8.544E+05	2.840E+04
$Q_{pot}\ (J)$	8.2947E+07	-	-
$E_a\ (kJ/mol)$	37.31	-	-
$A\ (W)$	4.9885E+09	-	-

Convective boundaries	
Convection coefficient (W/m²K)	15.250

b)

Figure 5: a) 3D view of the simulation model; b) Main parameters used for the numerical simulation

4.2. Thermo-mechanical simulation of the 21st construction phase

The numerical simulation of stresses developed in the 21st construction phase demanded the consideration of the entire height of construction up to this phase in order to simulate realistic conditions of restraint to deformation, as well as the thermal exchanges between hardening and hardened concrete. Bearing in mind that thermal exchanges also occur along horizontal planes (both longitudinal and transverse), the necessity for a 3D model for simulation is clearly established. Even though a realistic simulation would also demand the full construction schedule to be taken into account, thus leading to the necessity of a phased analysis, it was decided to make a simplification on this matter and perform an analysis that only comprises the 21st phase, assuming that all the preceeding phases have already attained thermal equilibrium with the environment. Even though such assumption may not hold entirely true, it is not far from reality, and the corresponding benefits in terms of computational cost are rather significant.

Another important topic regarding the overall modelling strategy is the consideration of the cooling tubes. The model shown here corresponds to a first attempt of modelling in which it was decided to not include specific cooling tube elements [20, 21]. Therefore, the tubes were modelled as hollow parts of concrete in which convective boundaries were considered. The temperature input to the tube boundaries was obtained from the monitoring at section A-A', which is thus only actually correct for section A-A' due to the heating effect that concrete has on the circulating air. It was nonetheless considered that this simplification was acceptable for a first trial, mainly bearing in mind that most sensors where placed at the section A-A'. However, it should be beard in mind that the trustworthiness of results in sections away from A-A' is reduced.

A schematic cross section of the 3D model can be seen in Figure 6a, where a colour description of the considered boundaries is made (valid throughout the entire 3D model). The distinct boundary coefficients correspond to: (a) concrete in direct contact with the surrounding environment, for which a convection coefficient h = 15 W m^{-2} K^{-1} is considered; (b) coincides with the symmetry plane, where no heat flux occurs; (c) for surfaces in contact with the formwork of the 21st phase, with adoption of h = 6.0 W m^{-2} K^{-1}; (d) cooling pipes, where h = 30.0 W m^{-2} K^{-1} was adopted during the time of forced ventilation and null in the other instants. The initial temperature for concrete was considered to be

14.5ºC for the 21st casting phase, and 10.3ºC for the previously existing concrete (in correspondence to the average environmental temperature of the 3 preceding days).

The finite element mesh has slight differences in terms of number of nodes per element for thermal and mechanical analyses, even though the corner nodes of the elements are always coincident. The thermal analysis uses 8 node solid elements for concrete (2×2×2 integration scheme) and 4 node planar elements for boundary elements (2×2 integration). The elements for mechanical analysis for concrete are 20 node solid elements with 3×3×3 integration scheme. The finite element mesh adopted for calculations has a total of 25537 nodes and 7116 elements, and it is represented in Figure 6b.

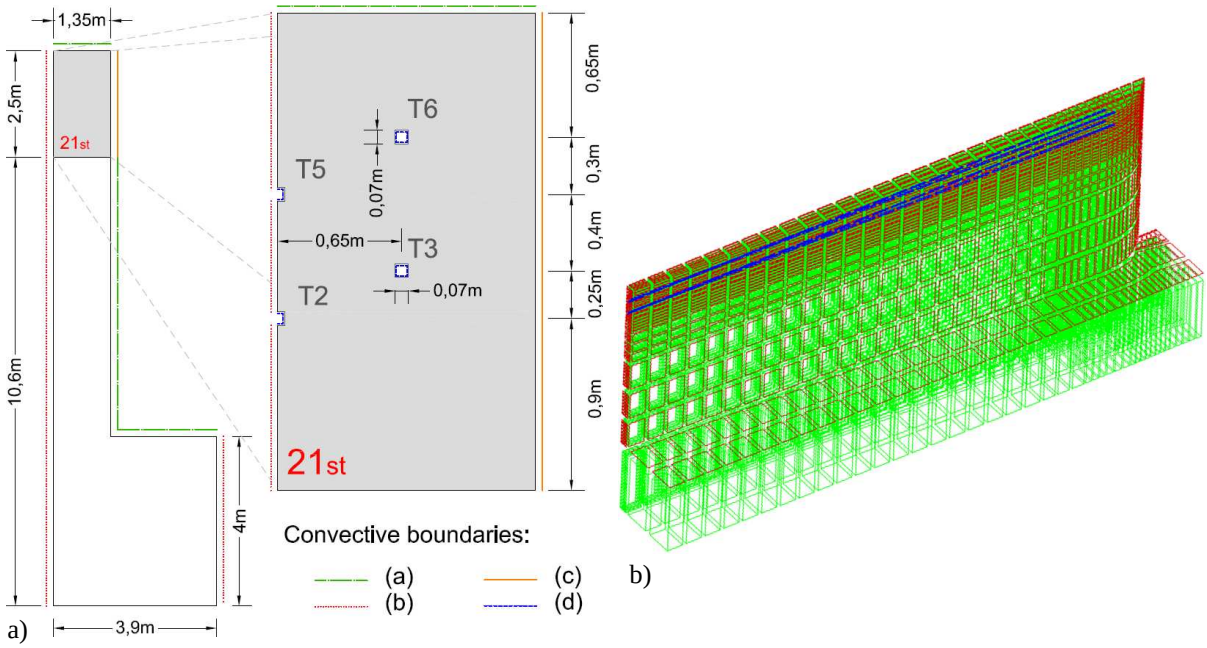

Figure 6: a) Schematic cross-section of the FE model; b) 3D view of the adopted mesh

The thermal properties of concrete in the model were considered to be the same as those described in Section 4.1. Mechanical properties were considered according to the data shown in sections 3.2 and 3.3, namely in what regards to: evolution of E-modulus and tensile strength; creep; equivalent age computation. Poisson's coefficient was considered constant with the value of 0.2. Finally, in regard to support conditions of the mechanical model, symmetry supports were considered in the symmetry plane, and vertical supports were considered below the bottommost horizontal surface of the model (where one of the nodes was also longitudinally restrained to assure equilibrium in such direction).

Due to space limitations, only some of the main results are shown, both in terms of thermal and mechanical analyses. In regard to the temperature simulations, it is worth discussing the simulation results (and corresponding monitored temperatures) at the location of sensors CV1 (located near the bottom boundary of the 21st phase) and CV5 (see locations in Figure 2b) as shown respectively in Figures 7a and 7b. A good coherence is obtained in both sensors during the temperature rise period, having however a slight underestimation of heat loss, particularly in sensor CV1. This may be related to the simplification of ignoring the construction phasing, which may have led to inaccuracies in the temperature field below the casting phase under study. A remark is given to the fact that the calculated temperatures at the location of the other temperature sensors had similar coherences, thus pointing to the feasibility of the temperature simulation at the vicinity of section A-A'. In regard to the efficiency of the cooling pipes at section A-A', it can be assessed by comparing the numerical results with those that would be obtained without consideration of cooling pipes. The temperature rise in sensor CV5 (one of the hotter regions of the model), which amounted to ~25ºC with cooling pipes, would have amounted to ~30ºC if pipes had not been used. Even though this is a non-negligible improvement, the effectiveness of cooling pipes would have been higher if a different configuration had been adopted: more pipes, with less development of each pipe along concrete. In fact, the air inside the pipes that were used in this wall was significantly heated along its path (e.g. from ~13ºC at its entrance to ~35ºC at its end at the age of 24 hours), thus limiting its capacity of cooling concrete.

Mechanical simulation results have to be validated taking the measured strains. Before showing such results, a brief comment is made in regard to the actually measured strains. Due to uncertainties about the instant at which the strain gage is actually fully solidarized to concrete, zeroing the sensor's output is difficult (as before full solidarization, the sensor is actually just measuring its free deformation). Therefore, in the presentation of results, it was decided to make a vertical shifting of each sensor's output as to match the peak numerically simulated strain. The corresponding results for sensors CV1 and CV5 are shown in Figure 8. It can once again be confirmed that reasonable coherences are obtained, pointing to the feasibility and realism of the numerical simulations.

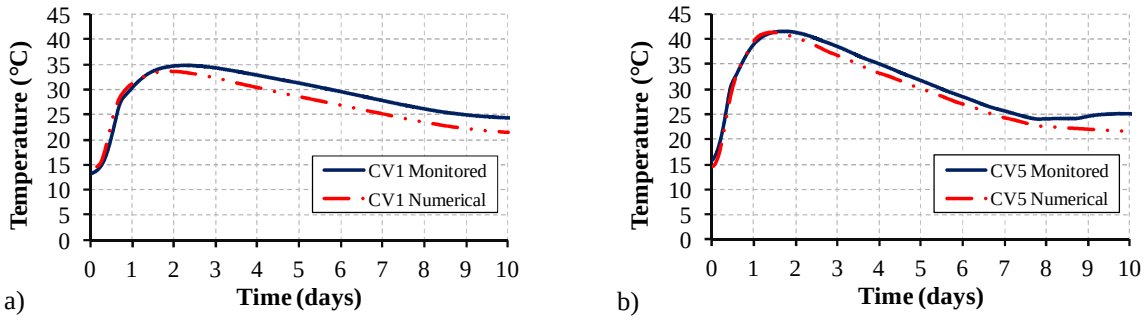

Figure 7: Monitored and calculated temperature evolutions at the locations of sensors: a) CV1; b) CV5

In view of the feasibility of the numerically obtained temperatures and stresses in comparison to monitored results, it can be argued that stress predictions of the model are bound to be realistic. Even though such detailed discussion cannot be made in this paper, some brief notes are given. The calculated stresses and their comparison to the evolving tensile strength of concrete has led to the conclusion that surface cracking risk was relatively low in the 21st phase, and that the risk of internal cracking upon cooling of concrete was significant, but circumscribed to relatively small core areas. Therefore, upon what has been stated, no visible thermal cracking was expectable for the construction in view of the numerical simulation. Such absence of cracking has been confirmed by visual inspection of the wall both during and after construction.

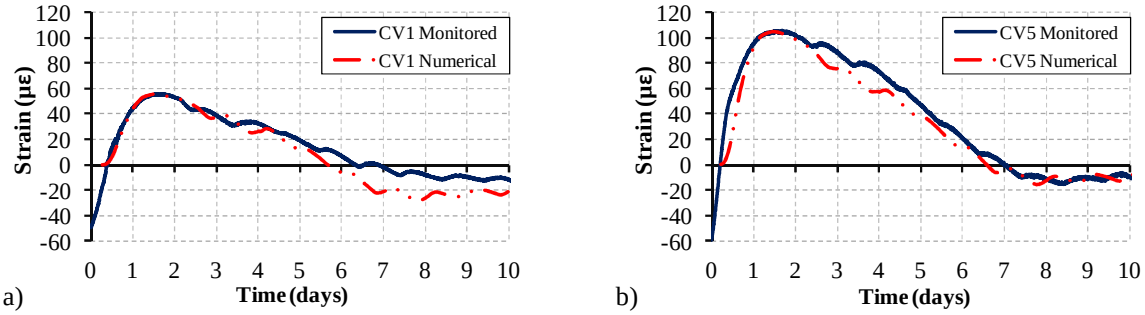

Figure 8: Monitored and calculated strain evolutions at the locations of sensors: a) CV1; b) CV5

5. Conclusions

The thermo-mechanical simulation of the central wall of the entrance of a dam spillway has been presented in this paper. The numerical simulation has been backed by extensive material characterization, and positively validated by comparisons with the results of an in-situ monitoring program that included temperature and strain measurements. The case study had added interest in view of the use of air-cooled pipes to diminish temperature development in concrete. The presented validation of numerical models and parameter characterization show a good level of confidence of current practices for cracking risk evaluation in mass concrete. In view of the simplified approach adopted for simulation of the cooling pipes (imposed air temperatures), further improvements to the numerical model regard the explicit modeling of the air flow inside the pipes and evaluation of its interaction with the surrounding concrete.

Acknowledgements

Funding provided by the Portuguese Foundation for Science and Technology to the Research Unit ISISE, as well as to the second author through the PhD grant SFRH/BD/64415/2009, and to the research project PTDC/ECM/099250/2008 is gratefully acknowledged. The kind assistance of the contractor (Teixeira Duarte SA) and the owner (EDP – Electricidade de Portugal) are also appreciated.

References

[1] M. Azenha, Numerical Simulation of the Structural Behaviour of Concrete Since its Early Ages, PhD Thesis, Faculty of Engineering, University of Porto, 2009.

[2] J.-E. Jonasson, Modelling of Temperature, Moisture and Stresses in Young Concrete, Doctoral Thesis, Lulea, Lulea University of Technology, 1994.

[3] L. Buffo-Lacarrière, A. Sellier, A. Turatsinze, G. Escadeillas, Finite element modelling of hardening concrete: application to the prediction of early age cracking for massive reinforced structures, Materials and Structures, 44 (2011) 1821-1835.

[4] G. De Schutter, Finite element simulation of thermal cracking in massive hardening concrete elements using degree of hydration based material laws, Computers & Structures, 80 (2002).

[5] H. Reinhardt, J. Blaauwendraad, J. Jongedijk, Temperature development in concrete structures taking account of state dependent properties., in: International Conference Concrete at Early Ages, Paris, France, 1982.

[6] F. Branco, P. Mendes, E. Mirambell, Heat of hydration effects in concrete structures, ACI Materials Journal, 89 (1992) 139-145.

[7] M. Larson, Thermal crack estimation in early age concrete models and methods for practical application, Doctoral Thesis, Luleå University Of Technology, 2003.

[8] P. Laplante, C. Boulay, Evolution du coefficient de dilatation thermique du béton en fonction de sa maturité aux tout premiers âges, Materials and Structures, 27 (1994) 596-605.

[9] O. Bjontegaard, E.J. Sellevold, Interaction between thermal dilation and autogenous deformation in high performance concrete, Materials and Structures, 34 (2001).

[10] M. Viviani, B. Glisic, I.F.C. Smith, Separation of thermal and autogenous deformation at varying temperatures using optical fiber sensors, Cement and Concrete Composites, 29 (2007) 435-447.

[11] Z. Bažant, E. Osman, Double power law for basic creep of concrete, Materials and Structures, 9 (1976) 3-11.

[12] R. Faria, M. Azenha, J.A. Figueiras, Modelling of concrete at early ages: Application to an externally restrained slab, Cement and Concrete Composites, 28 (2006) 572-585.

[13] M. Azenha, R. Faria, Temperatures and stresses due to cement hydration on the R/C foundation of a wind tower-A case study, Engineering Structures, 30 (2008) 2392-2400.

[14] H. Hedlund, P. Groth, Air cooling of concrete by means of embedded cooling pipes-Part I: Laboratory tests of heat transfer coefficients, Materials and Structures, 31 (1998) 329-334.

[15] CEN, EN 1992-1 European Standard Eurocode 2: Design of concrete structures - Part 1: general rules and rules for buildings, in, 2004.

[16] L. D'Aloia, G. Chanvillard, Determining the “apparent” activation energy of concrete: Ea—numerical simulations of the heat of hydration of cement, Cement and Concrete Research, 32 (2002) 1277-1289.

[17] M. Azenha, F. Magalhães, R. Faria, A. Cunha, New method for continuous monitoring of concrete E-modulus since casting using an output-only modal identification technique, in: Sixth Int Conference on Concrete under Severe Conditions - CONSEC'10, , Yucatan, Mexico, 2010.

[18] R. Aguilar, Dynamic Structural Identification using Wireless Sensor Networks, PhD Thesis, Civil Engineering, University of Minho, 2010.

[19] Â.M.V. Costa, Thermo-mechanical analysis of self-induced stresses in concrete associated to heat of hydration: a case study of the spillway of Paradela dam, Master Thesis, Civil Engineering, University of Minho, 2011 [in Portuguese].

[20] J.K. Kim, K.H. Kim, J.K. Yang, Thermal analysis of hydration heat in concrete structures with pipe-cooling system, Computers and Structures, 79 (2001) 163-171.

[21] T.G. Myers, N.D. Fowkes, Y. Ballim, Modeling the cooling of concrete by piped water, Journal of Engineering Mechanics, 135 (2009) 1375-1383.